First encounters on combs

Junhao Peng [1,2] and Elena Agliari [3,4]

[1]*School of Math and Information Science, Guangzhou University, Guangzhou 510006, China*

[2]*Guangdong Provincial Key Laboratory co-sponsored by province and city of Information Security Technology, Guangzhou University, Guangzhou 510006, China*

[3]*Department of Mathematics, Sapienza Università di Roma, 00185 Rome, Italy*

[4]*Istituto Nazionale di Alta Matematica, 00185 Rome, Italy*

(Received 4 October 2019; published 20 December 2019)

We consider two random walkers embedded in a finite, two-dimension comb and we study the mean first-encounter time (MFET) evidencing (mainly numerically) different scalings with the linear size of the underlying network according to the initial position of the walkers. If one of the two players is not allowed to move, then the first-encounter problem can be recast into a first-passage problem (MFPT) for which we also obtain exact results for different initial configurations. By comparing MFET and MFPT, we are able to figure out possible search strategies and, in particular, we show that letting one player be fixed can be convenient to speed up the search as long as we can finely control the initial setting, while, for a random setting, on average, letting one player rest would slow down the search.

DOI: 10.1103/PhysRevE.100.062310

I. INTRODUCTION

Nature displays many examples of comblike structures, such as comb polymers, nanowires, and spiny dendrites (see e.g., Refs. [1–3]). Artificial examples also abound: In several buildings and devices, such as antennas and probes, we can recognize a characteristic comb shape.

Mathematically, a comb can be described as a graph with vertex set $\mathbb{Z} \times \mathbb{Z}$ and edge set $\{[(x, y), (x, y')] : |y - y'| = 1\} \cup \{[(x, 0), (x', 0)] : |x - x'| = 1\}$; otherwise stated, the graph is obtained by taking a linear chain $\mathbb{Z}$ (also called backbone) and by attaching to each of its vertices another chain $\mathbb{Z}$. From this definition, many variations on theme also follows: d-dimension combs are obtained by attaching to each vertex in the side chain another chain; "wedge combs" are obtained by introducing a function $f : \mathbb{Z} \to \mathbb{Z}$ which controls the length of the side chains; "brushes" are obtained by replacing the backbone with a square lattice $\mathbb{Z}^2$; and, in general, branched structures can be obtained by attaching to each node of an arbitrary graph a chain (see, e.g., Refs. [4,5]). Of course, for practical applications one may be interested in finite combs where the infinite chains are replaced by finite chains of length L.

Over the past few decades these objects have been the subject of intensive studies, especially in relation to the properties of random walkers placed therein. For instance, if we are simply interested in the projection of the walker position on the backbone, then we can map the problem into a one-dimensional continuous-time random walk with a waiting-time distribution corresponding to the distribution of the time spent by the walker on a side chain of the original comb (see, e.g., Refs. [6–9]); accordingly, comblike models have also been used to mimic anomalous diffusion on fractal structures (see, e.g., Refs. [10–12]). Other works focused on the occupation time [13], on reaction-diffusion [14,15], and on propagator estimates [16], just to mention a few.

However, probably the most striking properties arise when dealing with two (or more) random walkers moving on the comb and looking for their encounters. In fact, infinite combs exhibit the so-called *finite collision* property (or *two-particle transience*), namely two independent walks meet only finitely many times (almost surely) [17,18]. This is rather unintuitive given that combs are recurrent, that is, a simple random walk visits infinitely many times any site of the structure. In other words, if a random walker is looking for a mobile target on a (infinite) comb, then there is a chance that the encounter will never occur, no matter how long we wait, while, if the target is fixed, then the random walker will surely find it eventually. Indeed, the two-particle transience and the one-particle recurrence are perfectly consistent and ultimately stem from the strong topological inhomogenity of the comb [5] (incidentally, we also recall the dimension splitting exhibited by combs [19]). Although these properties concern, by definition, infinite structures, some effects also emerge when the size is finite [20–22]: The mean first-encounter time (MFET), providing the characteristic time for the encounter when the target is mobile, can scale with the system size faster than the mean first-passage time (MFPT), providing the characteristic time for the encounter when the target is immobile. Again, this is qualitatively different from what one would intuitively expect having in mind a Euclidean lattice where MFET and MFPT display the same scaling and the possible quantitative difference would make the MFET smaller than the MFPT [23].

These findings suggest that search strategies on combs can be implemented: According to the situation (look, for instance, at the walkers as a predator and a prey or as two chemical reactants), it may be advantagous to making time for the two players to be on the same site—a condition that may trigger a certain event—either large or small [24].

In this work we address the problem of finding the best strategy in relation to the motion of the target and to the initial

 ©2019 American Physical Society

configuration. As we will see, a great variety of behaviors can occur and in order to settle a strategy it is crucial to have a suitable control of the initial setting.

This paper is structured as follows: In Sec. II we provide the main definitions and we describe the topology of the network considered. In Secs. III and IV we evaluate (average) MFET and MFPT, exploiting analytical and numerical methods and addressing different initial settings. In Sec. V we summarize results and, finally, Appendices A and B provide the technicalities on the calculations.

II. MAIN DEFINITIONS

A. Encounter times

The encounter time between two walkers A and B is the shortest time such that the two walkers are on the same site. In general, it depends on the underlying structure $\mathcal{S} = (V, E)$[1], on the initial position of the walkers $i_A, i_B \in V$, and on the particular realization of the walks. One typically treats $\mathcal{S}$ and (i_A, i_B) as parameters and looks for the related MFET, referred to as $\mathrm{MFET}^{\mathcal{S}}_{i_A,i_B}$. If A is fixed, then the MFET recovers the MFPT, similarly referred to as $\mathrm{MFPT}^{\mathcal{S}}_{i_A,i_B}$, where, again, (i_A, i_B) identifies the initial position of the walkers, but this time i_A never changes during the process.

Further, in order to get more synthetic information, one looks at the global-mean first-encounter time (GFET) obtained by averaging $\mathrm{MFET}^{\mathcal{S}}_{i_A,i_B}$ over all possible initial positions (i_A, i_B) drawn independently from the stationary distribution $\Pi = (\pi_1, \pi_2, \ldots, \pi_n)^T$, where $\pi_k = d_k / \sum_i d_i$, where d_k is the degree of the arbitrary vertex k in the structure $\mathcal{S}$. More precisely,

$$\mathrm{GFET}^{\mathcal{S}} := \sum_{i_A \in V} \sum_{i_B \in V} \pi_{i_A} \pi_{i_B} \mathrm{MFET}^{\mathcal{S}}_{i_A,i_B}. \tag{1}$$

However, when $i_A = i_B$, the probability that the node i is selected as the starting point for both A and B is taken as proportional to d_i^2 in such a way that

$$\mathrm{GFET}^{\mathcal{S}}_{i_A=i_B} := \sum_{i \in V} \frac{d_i^2}{\sum_k d_k^2} \mathrm{MFET}^{\mathcal{S}}_{i,i}. \tag{2}$$

We will also consider the case where i_A is fixed and the average is performed only on i_B, so to keep track of the effect of the target position, this quantity is defined as

$$\mathrm{GFET}^{\mathcal{S}}_{i_A} := \sum_{i_B \in V} \pi_{i_B} \mathrm{MFET}^{\mathcal{S}}_{i_A,i_B}. \tag{3}$$

Similarly, in the case where A is fixed, the MFPT taken by the walker B starting from i_B to first reach i_A, i.e., $\mathrm{MFPT}^{\mathcal{S}}_{i_A,i_B}$, can be averaged over all possible i_A, i_B drawn independently from the stationary distribution Π to get the global-average first-passage time (GFPT), that is,

$$\mathrm{GFPT}^{\mathcal{S}} := \sum_{i_A \in V} \sum_{i_B \in V} \pi_{i_A} \pi_{i_B} \mathrm{MFPT}^{\mathcal{S}}_{i_A,i_B}, \tag{4}$$

[1]As standard, V represents the set of vertices and E represents the set of edges.

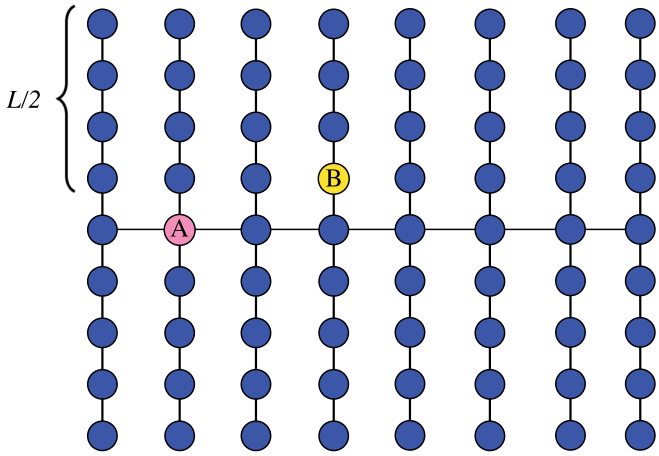

FIG. 1. Example of a two-dimension square comb. Here $L = 8$ and walkers A and B occur to be in the sites $(2, 0)$ and $(4, 1)$, respectively.

which is just Kemeny's constant and can be simplified as

$$\mathrm{GFPT}^{\mathcal{S}} := \sum_{i_A \in V} \pi_{i_A} \mathrm{MFPT}^{\mathcal{S}}_{i_A,i_B}. \tag{5}$$

The special case where $i_A = i_B = i$ corresponds to the mean return time and one has

$$\mathrm{GFPT}^{\mathcal{S}}_{i_A=i_B} := \sum_{i \in V} \frac{d_i^2}{\sum d_i^2} \mathrm{MFPT}^{\mathcal{S}}_{i,i}. \tag{6}$$

Finally, for a given i_A, averaging only on i_B,

$$\mathrm{GFPT}^{\mathcal{S}}_{i_A} := \sum_{i_B \in V} \pi_{i_B} \mathrm{MFPT}^{\mathcal{S}}_{i_A,i_B}. \tag{7}$$

B. The network structure

In this work we especially focus on two-dimensional square combs, which are built by fixing the length L (for simplicity L is even) of the backbone and by attaching to each of its sites two side chains of length $L/2$. In this way the total number of vertexes is

$$N := |V| = L(L + 1), \tag{8}$$

the total number of edges is

$$|E| = \frac{1}{2} \sum_{i \in V} d_i = (N - 1) = L^2 + L - 1, \tag{9}$$

and the mean-squared degree is

$$\sum_{i \in V} d_i^2 = 4L^2 + 10L - 14. \tag{10}$$

Each vertex can be indexed by (x, y) ($1 \leqslant x \leqslant L$ and $-\frac{L}{2} \leqslant y \leqslant \frac{L}{2}$), where x represents the location on the backbone and y represents the location on the teeth, see Fig. 1 for a sketch.

In the following we will refer to this kind of structure as $\mathcal{C} := \mathcal{C}(L)$.

III. GFET AND GFPT

In this section we focus on global averages for the MFET and MFPT specifying different initial settings.

A. Players starting from the same site

Here we consider a system where two players are initially set at the same site; we initially face the problem analytically for an arbitrary graph, and then we will apply the general result to the case of two-dimensional combs.

Let A and B denote two independent simple random walks on a graph $\mathcal{G} = (V, E)$ that is arbitrary, but finite, connected, and *not bipartite*. The two walkers start from the same site and, at each step, they move to any of their nearest neighbors with equal probability; we denote with $P = (p_{i,j})_{N\times N}$ the transferring probability matrix.

The first encounter time $T_{i,j}$ of two walkers starting from node i and node j, respectively, satisfies the following recursive formula [25]:

$$T_{i,j} = \begin{cases} 1 & \text{w.p.} \quad \sum_k p_{i,k}p_{j,k} \\ T_{k,h} + 1 & \text{w.p.} \quad p_{i,k}p_{j,h} (k \neq h) \end{cases}, \tag{11}$$

where w.p. is the abbreviation of "with probability." Then, posing $\text{MFET}^{\mathcal{G}}_{i,j} = m_{i,j}$ for any $i, j = 1, 2, \ldots, N$, to lighten the notation, one has

$$m_{i,j} = 1 + \sum_{k\neq h} p_{i,k}p_{j,h}m_{k,h}. \tag{12}$$

Also, introducing the matrix $M = (m_{i,j})_{N\times N}$, we can write

$$M = \mathbf{1}_N\mathbf{1}_N^T + P(M - M_d)P^T, \tag{13}$$

where $\mathbf{1}_N$ is the column vector of length N with entries all equal to 1 and M_d is the $N \times N$ diagonal matrix with kth entry equal to $m_{k,k}$. Recalling that $\Pi = (\pi_1, \pi_2, \ldots, \pi_n)^T$ is the stationary distribution for random walks and, by definition, $\Pi^T P = \Pi^T$, exploiting (13), we have

$$\begin{aligned} \Pi^T M \Pi &= \Pi^T \mathbf{1}_n\mathbf{1}_n^T \Pi + \Pi^T P(M - M_d)P^T \Pi \\ &= 1 + \Pi^T (M - M_d)\Pi. \end{aligned}$$

Thus, $\Pi^T M_d \Pi = 1$, or, more explicitly,

$$\sum_k \pi_k m_{k,k} \pi_k = 1. \tag{14}$$

The GFET for nonbipartite connected graphs where both players perform a random walk starting from the same site, defined in (2), therefore reads as

$$\text{GFET}^{\mathcal{G}}_{i_A=i_B} = \sum_i \frac{d_i^2}{\sum_k d_k^2} m_{i,i} = \frac{(2|E|)^2}{\sum_i d_i^2}. \tag{15}$$

We now consider a finite, connected *bipartite* graph $\mathcal{B} = (V, E)$ where the vertex set V can be decomposed into two disjoint subsets (i.e., $V = V_1 \cup V_2$) such that vertices belonging to the same subset are never adjacent, that is, $p_{i,j} = 0$, if i, j belong to the same subset. Moreover, one has

$$\sum_{k\in V_1} \pi_k = \sum_{k\in V_2} \pi_k = \frac{1}{2}. \tag{16}$$

If A starts from vertex i, B starts from vertex j, and i, j belong to different subsets (e.g., $i \in V_1$ and $j \in V_2$), then they can never meet and $m_{i,j} = \infty$[2]. If i and j belong to the same subset (e.g., $i \in V_1$ and $j \in V_1$), then

$$m_{i,j} = 1 + \sum_{k\in V_2} \left[p_{i,k} \sum_{h\in V_2} p_{j,h}m_{k,h} \right] - \sum_{k\in V_2} p_{i,k}p_{j,k}m_{k,k}.$$

Multiplying this expression by Π on the left and on the right, we get

$$\begin{aligned} \sum_{i\in V_1}\sum_{j\in V_1} \pi_i m_{i,j} \pi_j &= \sum_{i\in V_1} \pi_i \sum_{j\in V_1} \pi_j - \sum_{i\in V_1}\sum_{j\in V_1}\sum_{k\in V_2} \pi_i p_{i,k}p_{j,k}\pi_j m_{k,k} \\ &\quad + \sum_{i\in V_1}\sum_{j\in V_1}\sum_{k\in V_2}\sum_{h\in V_2} (\pi_i p_{i,k}p_{j,h}m_{k,h}\pi_j) \\ &= \frac{1}{4} - \sum_{k\in V_2} \pi_k m_{k,k}\pi_k + \sum_{k\in V_2}\sum_{h\in V_2} \pi_k m_{k,h}\pi_h. \end{aligned} \tag{17}$$

Of course, *mutatis mutandis*,

$$\sum_{i\in V_2}\sum_{j\in V_2} \pi_i m_{i,j} \pi_j = \frac{1}{4} - \sum_{k\in V_1} \pi_k m_{k,k}\pi_k + \sum_{k\in V_1}\sum_{h\in V_1} \pi_k m_{k,h}\pi_h. \tag{18}$$

By summing together (17) and (18),

$$\begin{aligned} &\sum_{i\in V_1}\sum_{j\in V_1} \pi_i m_{i,j} \pi_j + \sum_{i\in V_2}\sum_{j\in V_2} \pi_i m_{i,j} \pi_j \\ &\quad = \frac{1}{2} + \sum_{k\in V_1}\sum_{h\in V_1} \pi_k m_{k,h}\pi_h + \sum_{k\in V_2}\sum_{h\in V_2} \pi_k m_{k,h}\pi_h \\ &\quad\quad - \sum_{k\in V} \pi_k m_{k,k}\pi_k, \end{aligned} \tag{19}$$

whence $\sum_{k\in V} \pi_k m_{k,k}\pi_k = 1/2$. Therefore, following definition (2),

$$\text{GFET}^{\mathcal{B}}_{i_A=i_B} = \frac{1}{2}\frac{(2|E|)^2}{\sum_i d_i^2}. \tag{20}$$

If the target is not moving, then the encounter time recovers the return time and, for any finite, connected graph the mean first-return time to a node i is [26]

$$\text{MFPT}^{\mathcal{G},\mathcal{B}}_{i_A=i_B} = \frac{\sum_k d_k}{d_i}, \tag{21}$$

no matter whether the underlying structure is bipartite or not. Thus, plugging (21) into definition (6), the GFPT turns out to be

$$\text{GFPT}^{\mathcal{G},\mathcal{B}}_{i_A=i_B} = \frac{(2|E|)^2}{\sum_i d_i^2}. \tag{22}$$

[2]With a little rearranging, seeking a lighter notation and to avoid proliferation of symbols, we shall pose again $\text{MFET}^{\mathcal{B}}_{i,j} = m_{i,j}$ for any $i, j = 1, 2, \ldots, N$.

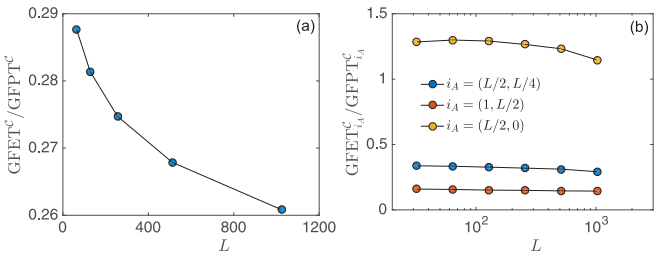

FIG. 2. (a) The ratio $\mathrm{GFET}^{\mathcal{C}}/\mathrm{GFPT}^{\mathcal{C}}$ is shown as a function of L; data for $\mathrm{GFET}^{\mathcal{C}}$ are obtained by numerical simulations, while data for $\mathrm{GFPT}^{\mathcal{C}}$ are obtained by evaluating the exact expression (27). Notice that the ratio $\mathrm{GFET}^{\mathcal{C}}/\mathrm{GFPT}^{\mathcal{C}}$ monotonically decreases with L and this allows us to derive that the move of walker A overall fastens the process and that, recalling that $\mathrm{GFPT}^{\mathcal{C}} \sim L^3$, $\mathrm{GFET}^{\mathcal{C}}/L^3$ scales sublinearly with L. (b) The ratio $\mathrm{GFET}^{\mathcal{C}}_{i_A}/\mathrm{GFPT}^{\mathcal{C}}_{i_A}$ is shown as a function of L for different choices of i_A.

Consequently, comparing (15), (20), and (22), for a *nonbipartite* connected graph we have

$$\mathrm{GFPT}^{\mathcal{G}}_{i_A=i_B} = \mathrm{GFET}^{\mathcal{G}}_{i_A=i_B}, \tag{23}$$

namely the move of target A has no effect on the GFET, while on *bipartite* connected graphs,

$$\mathrm{GFPT}^{\mathcal{B}}_{i_A=i_B} = 2\,\mathrm{GFET}^{\mathcal{B}}_{i_A=i_B}, \tag{24}$$

namely the move of target A fastens the encounter between the two players. Otherwise stated, in nonbipartite finite connected graphs the motion of the target A has no effects on the (global) encounter time, while on bipartite finite connected graphs the motion of the target A halves the (global) encounter time.

The two-dimensional comb $\mathcal{C}$ described in Sec. II B is bipartite and, using (9) and (10), we can write

$$\mathrm{GFET}^{\mathcal{C}}_{i_A=i_B} = \frac{1}{2}\mathrm{GFPT}^{\mathcal{C}}_{i_A=i_B} = \frac{(L^2+L-1)^2}{2L^2+5L-7}, \tag{25}$$

that is,

$$\mathrm{GFPT}^{\mathcal{C}}_{i_A=i_B} > \mathrm{GFET}^{\mathcal{C}}_{i_A=i_B}. \tag{26}$$

B. Players starting from independently drawn sites

Here we analyze the case of players starting from sites i_A and i_B drawn independently from the stationary distribution Π on $\mathcal{C}$. In particular, we derive the GFET, obtained by averaging the MFET over all possible initial positions of A and B, as defined in Eq. (1) and the GFPT, obtained by averaging the MFPT over all possible initial positions of A and B, as defined in Eq. (4). By comparing the two quantities we will be able to see the effect of the target motion on the overall process.

The GFET is addressed by means of numerical simulations which evidence that $\mathrm{GFET}^{\mathcal{C}}/L^3$ scales sublinearly with L (see Fig. 2).

The GFPT is addressed analytically finding

$$\mathrm{GFPT}^{\mathcal{C}} = \frac{5L^5+6L^4-9L^3-3L^2+7L-3}{6L^2+6L-6} \sim L^3, \tag{27}$$

whose detailed derivation is presented in Appendix A.

Therefore, we can conclude that

$$\mathrm{GFPT}^{\mathcal{C}} > \mathrm{GFET}^{\mathcal{C}}, \tag{28}$$

and the move of target A fastens the encounter between A and B. This is also evidenced in Fig. 2(a).

Therefore the result (26) is preserved as the constraint $i_A = i_B$ is relaxed.

C. One player starting from a given site

Here we analyze the MFET in the case where the initial position of target A is chosen at $i_A \in V$, while the initial position i_B of B is randomly drawn from the stationary distribution Π, and we derive the GFET by averaging over i_B, as defined in (3). This result will be then compared to the GFPT obtained by keeping A fixed, as defined in (7).

The GFET is approached numerically for different choices of i_A; the cases considered suggest that GFET_{i_A}/L^3 scales sublinearly.

As for $\mathrm{GFPT}^{\mathcal{C}}_{i_A}$, we got exact results for arbitrary $i_A = (x_{i_A}, y_{i_A})$ as

$$\begin{aligned}\mathrm{GFPT}^{\mathcal{C}}_{i_A} = {} & \frac{4L^5+15L^4+12L^3+3L^2+5L-9}{6(L^2+L-1)} \\ & + 2x_{i_A}(1+L)(x_{i_A}-L-1 \\ & + 2|y_{i_A}|(|y_{i_A}|+L^2-1) \sim L^3,\end{aligned} \tag{29}$$

and the detailed derivation is presented in Appendix A. From (29) one can see that $\mathrm{GFPT}^{\mathcal{C}}_{i_A}$ increases with $|y_{i_A}|$ while $0 \leqslant |y_{i_A}| \leqslant L/2$. Also,

$$\frac{\partial}{\partial x_{i_A}}\mathrm{GFPT}^{\mathcal{C}}_{i_A} = 4x_{i_A}(L+1) - 2(L+1)^2, \tag{30}$$

that is, $\mathrm{GFPT}^{\mathcal{C}}_{i_A}$ is a convex function of $x_{i_A} \in [1, L/2]$ and it reaches its minimum at $i_A = (L/2, 0)$

$$\min_{i_A} \mathrm{GFPT}^{\mathcal{C}}_{i_A} = \frac{L^5+3L^4+6L^2+11L-9}{6L^2+6L-6},$$

and its maximum at $i_A = (1, \pm L/2)$ and at $i_A = (L, \pm L/2)$

$$\max_{i_A} \mathrm{GFPT}^{\mathcal{C}}_{i_A} = \frac{10L^5+12L^4-21L^3-6L^2+23L-9}{6L^2+6L-6}.$$

By looking at the ratio between $\mathrm{GFET}^{\mathcal{C}}_{i_A}$ and $\mathrm{GFPT}^{\mathcal{C}}_{i_A}$ (see Fig. 2, right panel), we find that if the distance between i_A and the central site $(L/2, 0)$ scales linearly with L,

$$\mathrm{GFPT}^{\mathcal{C}}_{i_A} > \mathrm{GFET}^{\mathcal{C}}_{i_A}, \tag{31}$$

namely if the initial position of the target (i.e., i_A) is far from the central site $(L/2, 0)$, its motion fastens the encounter; however, when i_A is close to the central site finite-size effects may yield to corrections.

A further representation is provided in Fig. 3, where we show a colormap for $\mathrm{GFET}^{\mathcal{C}}_{i_A}$ [Fig. 3(b)], for $\mathrm{GFPT}^{\mathcal{C}}_{i_A}$ [Fig. 3(b)], and for their logarithmic ratio [Fig. 3(c)]. In particular, notice that getting far from $i_A = (L/2, 0)$, $\mathrm{GFET}^{\mathcal{C}}_{i_A}/\mathrm{GFET}^{\mathcal{C}}_{i_A}$ moves from values that are larger than 1 to values that are smaller than 1.

IV. MFET AND MFPT

In this section we focus on the MFET and the MFPT specifying different initial settings.

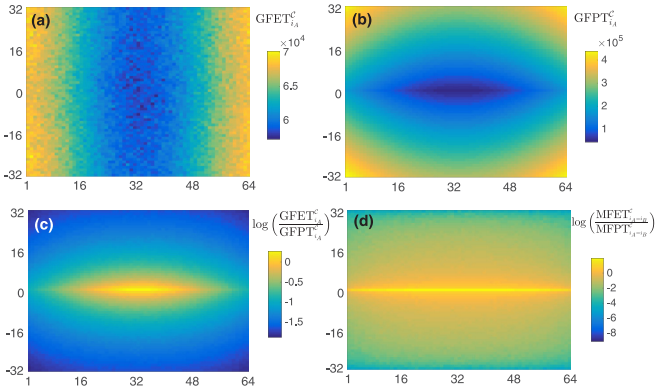

FIG. 3. Color map for $\mathrm{GFET}^{\mathcal{C}}_{i_A}$ (a), $\mathrm{GFPT}^{\mathcal{C}}_{i_A}$ (b), their logarithmic ratio (c) and the logarithmic ratio of $\mathrm{MFET}^{\mathcal{C}}_{i_A}$ and $\mathrm{MFPT}^{\mathcal{C}}_{i_A}$ (d). Each pixel represents a different choice of i_A in a comb of size $L = 64$; the brighter the color and the larger the related value according to the related legends. Data for GFPT and for MFPT stem for the exact formulas (22) and (33), while data for GFET and MFET stem from numerical simulations (in both cases averages are made over 10^5 realizations; statistical fluctuations are still rather evident for GFET).

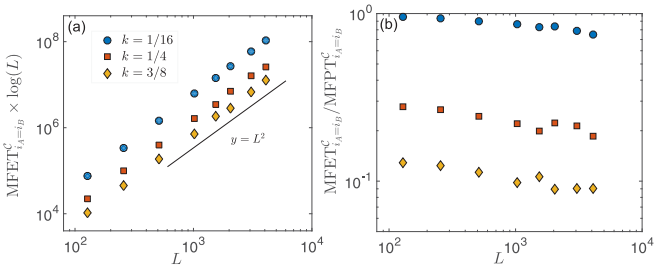

FIG. 4. (a) Numerical results for $\mathrm{MFET}^{\mathcal{C}}_{i_A=i_B,k>0}$ are analyzed to get evidence about the scaling (35); in particular, for different choices of $k > 0$ (as explained by the legend) we get that $\mathrm{MFET}^{\mathcal{C}}_{i_A=i_B,k>0} \times \log(L)$ scales as L^2 (the function $y = L^2$ is depicted in black as a reference). (b) The ratio $\mathrm{MFET}^{\mathcal{C}}_{i_A=i_B,k>0}/\mathrm{MFPT}^{\mathcal{C}}_{i_A=i_B,k>0}$ obtained by dividing numerical estimates for $\mathrm{MFET}^{\mathcal{C}}_{i_A=i_B,k>0}$ by the exact evaluation of $\mathrm{MFPT}^{\mathcal{C}}_{i_A=i_B,k>0}$ from (33) is plotted versus L for different choices of k (same legend as left panel). The decreasing trend confirms that $\mathrm{MFET}^{\mathcal{C}}_{i_A=i_B,k>0}$ scales less than quadratically with L and therefore, in this case, the motion of reactant A fastens the encounter.

A. Players starting from the same site

Here we initially set both players on a site labeled as (x_0, y_0) with $y_0 = kL$ $(0 \leqslant k \leqslant 1/2)$ on a two-dimensional comb. First, we address the case where the initial site belongs to the backbone (i.e., $k = 0$), and next is the case where it belongs to a tooth (i.e., $k > 0$).

1. Starting on the backbone

When $k = 0$ we can refer to previous results [21,22], which showed that the MFET for two walkers starting from a site in the backbone scales with the linear size L of the comb as

$$\mathrm{MFET}^{\mathcal{C}}_{\substack{i_A=i_B \\ k=0}} \sim \frac{L^3}{\log(L)}. \tag{32}$$

If the target is immobile, then the MFET is just the mean first return time for B. For any vertex (x_0, y_0) with $y_0 = 0$ in $\mathcal{C}$, the degree is 4 (or 3 for the end nodes). Then, recalling formula (21) and (9), the MFPT while A is immobile satisfies

$$\mathrm{MFPT}^{\mathcal{C}}_{\substack{i_A=i_B \\ k=0}} = \frac{1}{2}(L^2 + L - 1), \tag{33}$$

[or $\mathrm{MFPT}^{\mathcal{C}}_{\substack{i_A=i_B \\ k=0}} = 2(L^2 + L - 1)/3$ for the end nodes]. Therefore, as long as L is large enough,

$$\mathrm{MFPT}^{\mathcal{C}}_{\substack{i_A=i_B \\ k=0}} < \mathrm{MFET}^{\mathcal{C}}_{\substack{i_A=i_B \\ k=0}}, \tag{34}$$

which means that if A and B start at the same vertex in the backbone, then the move of A slows down the encounter.

2. Starting on the teeth

When $y_0 = kL$ $(0 < k < 1/2)$, we can figure out two possible scenarios: (i) the first encounter between A and B happens before one of the two walkers leaves the tooth that they both start from, and (ii) the first encounter between A and B happens after one of the two walkers leaves the tooth they both start from. Therefore, the overall MFET can be written as the sum of the MFETs related to case (i) and to case (ii), weighted by the probability that, respectively, case (i) and case (ii) occurs.

The first scenario can be looked on as the encounter problem on a finite one-dimensional interval $[0, L/2]$ with absorbing boundary at site 0 and a reflecting boundary at $L/2$, while both A and B start at y_0 with $y_0 = kL$ $(0 < k < 1/2)$. The probability P_{exit} that one of the two walkers leaves the common tooth before encounter is just the probability that one of the two walkers is absorbed at 0 before they encounter on a finite one-dimensional interval $[0, L/2]$.

Previous results [27–29] showed that $P_{\mathrm{exit}} \sim y_0^{-1} \sim L^{-1}$ and the MFET before one of the two particles is absorbed on a finite one-dimensional interval scales linearly with the length of the interval.

As for the second scenario, the MFET is by far longer as it takes a time scaling as $L^3/\log(L)$ [21,22], therefore providing the leading contribution for the overall MFET that reads as

$$\mathrm{MFET}^{\mathcal{C}}_{\substack{i_A=i_B \\ k>0}} \sim \frac{L^2}{\log(L)}. \tag{35}$$

This result is corroborated by numerical simulations: in Fig. 4(a), the quantity $\mathrm{MFET} \times \log(L)$ is shown to scale quadratically with L for different choices of the initial site. We also notice that $\mathrm{MFET}^{\mathcal{C}}_{\substack{i_A=i_B \\ k>0}}$ decreases with k, that is, the larger the initial distance from the backbone and the smaller the MFET.

Let us now face the case where the target A is immobile, that is, we look at the mean first return time of B. Recalling (21), (9), and the fact that for any vertex (x_0, y_0) in $\mathcal{C}$ with $y_0 = kL$ $(0 < k < 1/2)$ the degree is 2, we get

$$\mathrm{MFPT}^{\mathcal{C}}_{\substack{i_A=i_B \\ k>0}} = L^2 + L - 1. \tag{36}$$

Then, comparing (35) and (36), as long as L is large enough, we can state that

$$\mathrm{MFPT}^{\mathcal{C}}_{\substack{i_A=i_B \\ k>0}} > \mathrm{MFET}^{\mathcal{C}}_{\substack{i_A=i_B \\ k>0}}. \tag{37}$$

This result is corroborated by Fig. 4 (right panel) which shows the ratio between the numerical results for $\mathrm{MFET}_{\substack{i_A=i_B\\k>0}}$ and the exact result for $\mathrm{MFPT}^{\mathcal{C}}_{\substack{i_A=i_B\\k>0}}$ is decreasing with L and this effect is enhanced far larger values of k.

Further insights are provided in Fig. 3(d), where one can see that, when i_A is relatively far from the backbone, the MFET can be much smaller than the MFPT.

Finally, for the case $k = 1/2$, the vertex (x_0, y_0) is just a node with degree 1, and therefore the MFET is just 1, while, in general, the MFPT is larger than 1, in such a way that, also for this case, the move of target A fastens the encounter between A and B:

$$\mathrm{MFPT}^{\mathcal{C}}_{\substack{i_A=i_B\\k=1/2}} > \mathrm{MFET}^{\mathcal{C}}_{\substack{i_A=i_B\\k=1/2}}. \tag{38}$$

In conclusion, we obtain that if A and B start at the same vertex in a tooth and the distance from the vertex to the backbone is relatively large, the move of target A fastens the encounter between A and B.

B. Players starting from different sites

Here we consider the case where A and B start from arbitrary, fixed sites i_A and i_B on $\mathcal{C}$ and we derive the related MFPT and MFET.

The latter is addressed numerically via simulations obtaining a scaling with respect to L which ranges from L^3 (if the initial distance between walkers is relatively large, namely $\sim L$ [22]) to $L^2/\log L$ (if walkers are initially on the same tooth and relatively far from the backbone).

As for the MFPT, its evaluation is addressed analytically finding exact results. In particular, specifying the initial position of reactants in terms of the position along the backbone and along the tooth, that is, setting $i_A = (x_{i_A}, y_{i_A})$ and $i_B = (x_{i_B}, y_{i_B})$, we get

$$\begin{aligned}\mathrm{MFPT}^{\mathcal{C}}_{\substack{i_A,i_B\\x_{i_A}\neq x_{i_B}}} &= 2|y_{i_A}|(L^2-1) + L(|y_{i_B}| + |y_{i_A}|)\\ &\quad + y_{i_A}^2 - y_{i_B}^2 + (L^2+L-1)|x_{i_B} - x_{i_A}|\\ &\quad + (x_{i_A} - x_{i_B})(L+1)(x_{i_A} + x_{i_B} - L - 1)\end{aligned} \tag{39}$$

and

$$\begin{aligned}\mathrm{MFPT}^{\mathcal{C}}_{\substack{i_A,i_B\\x_{i_A}=x_{i_B}}} &= (L^2+L-1)|y_{i_A} - y_{i_B}|\\ &\quad + (|y_{i_A}| - |y_{i_B}|)(L^2 - 1 + |y_{i_A}| + |y_{i_B}|).\end{aligned} \tag{40}$$

The detailed derivations of Eqs. (39) and (40) are based on the connection between the MFPT and the effective resistance (see, e.g., Refs. [30,31]) and are presented in Appendix B.

By comparing results for MFET and MFPT, we get that if A and B start from sites that are relatively close each other and to the backbone, then the motion of A slows down the process, namely the result of Sec. IV A [Eq. (36)] is robust against relatively small changes in the initial setting; on the other hand, when the distance between A and B is relatively large, the outcome sensitively depends on the specific initial configuration (see Fig. 5). In particular, when A and B are initially on the same tooth, with $y_{i_A} y_{i_B} > 0$ and then if the initial position of A is closer to the backbone than the initial position of B, then the move of target A slows the encounter between A and B and vice versa (see Fig. 6).

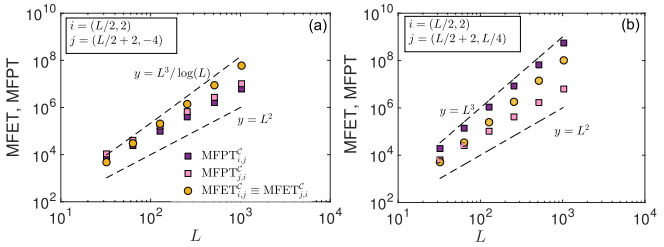

FIG. 5. Numerical results for $\mathrm{MFET}^{\mathcal{C}}_{i_A,i_B}$ and exact result for $\mathrm{MFPT}^{\mathcal{C}}_{i_A,i_B}$ are compared for different choices of the initial site. In particular, here $x_{i_A} \neq x_{i_B}$ and $|y_{i_A} - y_{i_B}|$ either does not scale with L (a) or it does scale with L (b). In the former case the move of target A slows the encounter, while in the latter case different scenarios are possibile according to the initial setting.

V. CONCLUSION

In this work we considered two "players," referred to as A and B, set on a two-dimensional comb structure and such that their encounter is able to trigger an event. The mean time to first encounter therefore provides the time scale for the event to occur. As outlined in previous works (see, e.g., Refs. [20–22]) this timescale can be significantly influenced by whether both players are moving or one, say, A, is fixed. Such information is crucial to design a strategy able to fasten or slow down, according to the specific problem, the process (see e.g., Refs [23,24,32]).

In this work we made a step forward by evidencing that the initial setting can also play a significant role. In fact, according to the initial position of A and B different scenarios can emerge as summarized by Table I. Therefore, in general, if the initial positions are set randomly, the motion of player A would, on average, speed up the process. However, if we are able to finely control the positions of both players (for instance placing them relatively close each other and to the backbone), then we can exploit the particular topology of the comb to get a slowdown of the process by letting both players move.

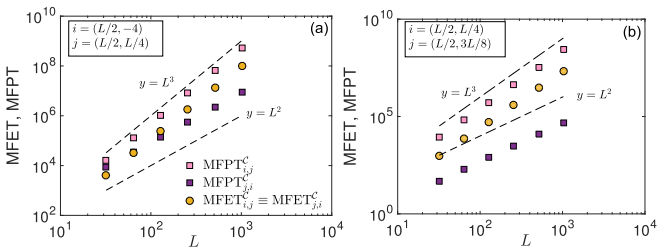

FIG. 6. Numerical results for $\mathrm{MFET}^{\mathcal{C}}_{i_A,i_B}$ and exact result for $\mathrm{MFPT}^{\mathcal{C}}_{i_A,i_B}$ are compared for different choices of initial site. In particular, here $x_{i_A} = x_{i_B}$. According to the initial setting the move of target A can either slow or fasten the encounter.

TABLE I. This table summarizes the main results of the work. Here $d(i, j)$ denotes the chemical distance between two nodes $i, j \in V$ and the big O notation is used to distinguish between quantities which scale (or do not scale) with the linear size L of $\mathcal{C}$ as L is grown larger and larger.

Initial state	Encounter times
$i_A = i_B \sim \Pi$	GFPT > GFET
$i_A, i_B \sim \Pi$	GFPT > GFET
$i_B \sim \Pi$	$\mathrm{GFPT}_{i_A} \lessgtr \mathrm{GFET}_{i_A}$
$d(i_A, i_B) \sim \mathcal{O}(1)$ and $y_A, y_B \sim \mathcal{O}(1)$	$\mathrm{MFPT}_{i_A,i_B} < \mathrm{MFET}_{i_A,i_B}$
$d(i_A, i_B) \sim \mathcal{O}(L)$	$\mathrm{MFPT}_{i_A,i_B} \lessgtr \mathrm{MFET}_{i_A,i_B}$

ACKNOWLEDGMENTS

J.P. is supported by the National Key R&D Program of China (Grant No. 2018YFB0803604), the National Natural Science Foundation of China (Grant No. 61873069 and 61772147), and the special innovation project of colleges and universities in Guangdong (Grant No. 2017KTSCX140). E.A. is grateful to Sapienza University of Rome (Progetto Ateneo RG11715C7CC31E3D and RM118164368D6841) for financial support.

APPENDIX A: DERIVATION OF EQS. (27) AND (29)

First, we report the derivation of Eq. (27). Substituting $\mathrm{MFPT}^{\mathcal{C}}_{i_A,i_B}$ into Eq. (5) with the right-hand side of Eq. (B1), we obtain

$$\begin{aligned}\mathrm{GFPT}^{\mathcal{C}} &= |E| \sum_{i_A \in V} \pi_{i_A} (L_{i_A,i_B} + W_{i_A} - W_{i_B}) \\ &= |E| \sum_{i_A \in V} \pi_{i_A} W_{i_A}. \end{aligned} \tag{A1}$$

Recalling the expression for W_j in Eq. (B4), we get

$$\begin{aligned}\sum_{j\in V} \pi_j W_j &= \sum_{j\in V} \frac{d_j}{2|E|} W_j \\ &= \sum_{j\in V} \frac{d_j}{8|E|^2}(3L^3 + 4L^2 + 2) \\ &\quad + \sum_{(x_j,y_j)\in V} \frac{d_j}{2|E|^2}[x_j^2 L - x_j L^2 - 2x_j L + x_j^2 - x_j] \\ &\quad + \sum_{(x_j,y_j)\in V} \frac{d_j}{2|E|^2}[L^2|y_j| + y_j^2 - |y_j|] \\ &= \frac{5L^5 + 6L^4 - 9L^3 - 3L^2 + 7L - 3}{6|E|^2}. \end{aligned} \tag{A2}$$

Inserting Eq. (A2) into Eq. (A1), we obtain Eq. (27).

Let us now derive the exact result of $\mathrm{GFPT}^{\mathcal{C}}_{i_A}$ [i.e., Eq. (29)] for arbitrary $i_A = (x_{i_A}, y_{i_A})$.

Recalling that for the arbitrary structure $\mathcal{S}$

$$\mathrm{MFPT}^{\mathcal{S}}_{i_A,i_B} = |E|(L_{i_A,i_B} + W_{i_A} - W_{i_B}),$$

and posing for simplicity $m_{i,j} := \mathrm{MFPT}^{\mathcal{C}}_{i,j}$, the GFPT can be expressed as [31]

$$\begin{aligned}\mathrm{GFPT}^{\mathcal{C}}_{i_A} &= \sum_{j\in V} \pi_j m_{i_A,j} = \pi_i m_{i_A,i_A} + \sum_{j\neq i_A} \pi_j m_{i_A,j} \\ &= 1 + \sum_{j\neq i_A} \pi_j |E|(L_{i_A,j} + W_{i_A} - W_j) \\ &= |E|(2W_{i_A} - \sum_{j\in V} \pi_j W_j) + 1. \end{aligned} \tag{A3}$$

Inserting Eqs. (A2) and (B4) into Eq. (A3), Eq. (29) is obtained.

APPENDIX B: DERIVATION OF EQS. (40) AND (39)

Here we calculate the MFPT from an arbitrary site j to an arbitrary site i on $\mathcal{C}$, exploiting the connection between the MFPT and the effective resistance (see, e.g., [30,31]). In fact, we can write

$$\mathrm{MFPT}^{\mathcal{C}}_{i,j} = |E|(L_{i,j} + W_i - W_j), \tag{B1}$$

where $L_{i,j}$ denotes the shortest-path length between vertex i and j, $|E|$ is the total number of edges, and W_j is the weighted average path length from any vertex to vertex j defined as

$$W_j = \sum_{i\in V} \pi_i L_{i,j} = \sum_{i\in V} \frac{d_i}{2|E|} L_{i,j}. \tag{B2}$$

For the two-dimensional comb described in Sec. II B, we find, for arbitrary sites $i = (x_i, y_i)$ and $j = (x_j, y_j)$,

$$L_{i,j} = \begin{cases} |y_j - y_i| & x_j = x_i \\ |y_j| + |y_i| + |x_j - x_i| & x_j \neq x_i \end{cases}. \tag{B3}$$

Inserting Eq. (B3) into Eq. (B2), for any vertex $j = (x_j, y_j)$, we get

$$\begin{aligned} W_j &= \frac{1}{2|E|} \sum_{i\in V} (L_{i,j} \cdot d_i) \\ &= \frac{1}{|E|} \Bigg\{ 2 \sum_{x_i=2}^{L-1} (|x_i - x_j| + |y_j|) + \frac{3}{2}(L-1) + 3|y_j| \\ &\quad + \sum_{y_i=1-L/2}^{L/2-1} |y_i - y_j| + L + \sum_{x_i\neq x_j} \left(2 \sum_{y_i=1}^{L/2-1} y_i + \frac{L}{2} \right) \\ &\quad + \sum_{x_i\neq x_j} [(|x_i - x_j| + |y_j|)(L-1)] \Bigg\} \\ &= \frac{1}{|E|} \Big\{ \frac{3}{4} L^3 + L^2 + \frac{1}{2} + y_j^2 \\ &\quad + (L+1)\big[x_j^2 - x_j(L+1) + |y_j|(L-1)\big] \Big\}. \end{aligned} \tag{B4}$$

Plugging Eqs. (B3) and (B4) into Eq. (B1), we obtain Eqs. (39) and (40).

Further, from Eqs. (39) and (40) we can highlight the following scalings:

(i) if $x_{i_A} \neq x_{i_B}$ (i.e., A and B start from a different tooth),

$$\mathrm{MFPT}^{\mathcal{C}}_{\substack{i_A,i_B \\ x_{i_A}\neq x_{i_B}}} \sim \begin{cases} L^3, & \text{if } |y_{i_A}| \sim L \text{ or } |x_{i_B} - x_{i_A}| \sim L \\ L^2, & \text{if } |y_{i_A}| \sim |x_{i_B} - x_{i_A}| \sim \text{const} \end{cases};$$

(ii) if $x_{i_A} = x_{i_B}$ and $y_{i_A} \times y_{i_B} \leqslant 0$ (i.e., A and B start from different sides of a tooth),

$$\mathrm{MFPT}^{\mathcal{C}}_{\substack{i_A,i_B \\ x_{i_A}=x_{i_B}}} \sim \begin{cases} L^3, & \text{if } |y_{i_A}| \sim L \\ L^2, & \text{if } |y_{i_A}| \sim \text{const} \end{cases}.$$

(iii) if $x_{i_A} = x_{i_B}$ and $y_{i_A} \times y_{i_B} \geqslant 0$ (i.e., A and B start from the same side of a tooth),

$$\mathrm{MFPT}^{\mathcal{C}}_{\substack{i_A,i_B \\ x_{i_A}=x_{i_B}}} \sim \begin{cases} L, & \text{if } |y_{i_B}| > |y_{i_A}|,\ |y_{i_B}| - |y_{i_A}| \sim \text{const} \\ L^2, & \text{if } |y_{i_B}| > |y_{i_A}|,\ |y_{i_B}| - |y_{i_A}| \sim L \\ L^2, & \text{if } |y_{i_B}| < |y_{i_A}|,\ |y_{i_A}| - |y_{i_B}| \sim \text{const} \\ L^3, & \text{if } |y_{i_B}| < |y_{i_A}|,\ |y_{i_A}| - |y_{i_B}| \sim L \end{cases}.$$

[1] J. Douglas, J. Roovers, and K. Freed, Macromolecules **23**, 4168 (1990).
[2] X. Fang, Y. Bando, U. Gautam, T. Zhai, H. Zeng, X. J. Xu, M. Liao, and D. Golberg, Crit. Rev. Solid State Mater. Sci. **34**, 190 (2009).
[3] R. Yuste, *Dendritic Spines* (MIT Press, Cambridge, MA, 2010).
[4] D. Cassi and S. Regina, Phys. Rev. Lett. **70**, 1647 (1993).
[5] E. Agliari and D. Cassi, First-passage phenomena on finite inhomogeneous networks, in *First-Passage Phenomena and Their Applications* (World Scientific Publishing, Singapore, 2004).
[6] S. Havlin, J. E. Kiefer, and G. H. Weiss, Phys. Rev. A **36**, 1403 (1987).
[7] G. H. Weiss and S. Havlin, Physica A **134**, 474 (1986).
[8] B. Durhuus, T. Jonsson, and J. F. Wheater, J. Phys. A **39**, 1009 (2006).
[9] D. Bertacchi, Electr. J. Probab. **11**, 1184 (2006).
[10] G. H. Weiss and S. Havlin, Philos. Mag. B **56**, 941 (1987).
[11] A. Iomin, V. Méndez, and W. Horsthemke, *Fractional Dynamics in Comb-like Structures* (World Scientific, Singapore, 2018).
[12] V. Arkhincheev, Chaos **17**, 043102 (2007).
[13] A. Rebenshtok, E. Barkai, Phys. Rev. E **88**, 052126 (2013).
[14] D. Campos and V. Méndez, Phys. Rev. E **71**, 051104 (2005).
[15] O. Bénichou, P. Illien, G. Oshanin, A. Sarracino, and R. Voituriez, Phys. Rev. Lett. **115**, 220601 (2015).
[16] P. Illien and O. Bénichou, J. Phys. A **49**, 265001 (2016).
[17] M. Krishnapur and Y. Peres, Elect. Comm. Probab. **9**, 72 (2004).
[18] M. T. Barlow, Y. Peres, and P. Sousi, Ann. l'Inst. Henri Poincaré **48**, 922 (2012).
[19] R.Burioni, D.Cassi, and S. Regina, Mod. Phys. Lett. B, **10**, 1059 (1996).
[20] R. Campari and D. Cassi, Phys. Rev. E **86**, 021110 (2012).
[21] E. Agliari, A. Blumen, and D. Cassi, Phys. Rev. E **89**, 052147 (2014).
[22] E. Agliari, D. Cassi, L. Cattivelli, and F. Sartori, Phys. Rev. E **93**, 052111 (2016).
[23] M. Moreau, G. Oshanin, O. Bénichou, and M. Coppey, Phys. Rev. E **67**, 045104(R) (2003).
[24] S. Redner, *A Guide to First-Passage Processes* (Cambridge University Press, Cambridge, UK, 2007).
[25] M. George, R. Patel, and F. Bullo, arXiv:1806.08843v1 (2018).
[26] L. Lovász, *Combinatorics: Paul Erdos is Eighty* (Keszthely, Hungary, 1993).
[27] D. Holcman and I. Kupka, J. Phys. A **42**, 1943 (2009).
[28] V. Tejedor, M. Schad, O. Bénichou, R. Voituriez, and R. Metzler, J. Phys. A **44**, 395005 (2011).
[29] A. Gabel, S. N. Majumdar, N. K. Panduranga, and S. Redner, J. Stat. Mech. (2012) P05011.
[30] J. H. Peng, J. Stat. Mech. (2014) P12018.
[31] J. H. Peng, G. A. Xu, R. X. Shao, C. Lin, and H. E. Stanley, J. Chem Phys. **149**, 024903 (2018).
[32] G. Oshanin, O. Vasilyev, P. Krapivsky, and J. Klafter, Proc. Natl. Acad. Sci. USA **106**, 13696 (2009).